

Regular and Chaotic Behaviors of Modified Rayleigh-Duffing oscillator

C. H. Miwadinou^{1*}, A. V. Monwanou^{1†}, C. Aïnamon^{2‡} and
J. B. Chabi Orou^{1,2§}

¹ Institut de Mathématiques et de Sciences Physiques, BP: 613 Porto Novo, Bénin,

² Ecole Doctorale Sciences des Matériaux, Université d'Abomey-Calavi, Bénin.

Abstract

The regular and chaotic behavior of modified Rayleigh-Duffing oscillator is studied. We consider in this paper the dynamics of Modified Rayleigh–Duffing oscillator. The harmonic balance method are used to find the amplitudes of the oscillatory states, and analyze. The influence of system parameters are clearly found on the bifurcations in the response of this system is investigated. It is found also hysteresis and jump phenomenon are appeared or disappeared when certain parameters increases or decreases. Various bifurcation structures, the variation of the Lyapunov exponent are obtained, using numerical simulations of the equations of motion. Various basin attraction are used to confirm the predictions of bifurcation structures and its corresponds Lyapunov exponent.

1 Introduction

In recent years, a twofold interest has attracted theoretical, numerical, and experimental investigations to understand the behavior of nonlinear oscillators. Theoretical (fundamental) investigations reveal their rich and complex behavior, and the experimental (self-excited oscillators) describes the evolution of many biological, chemical, physical, mechanical, and industrial systems [1, 2, 3]. The interest

*clement.miwadinou@imsp-uac.org, hodevewan@yahoo.fr

†movins2008@yahoo.fr

‡ainamoncyrille@yahoo.fr

§Author to whom correspondence should be addressed: jchabi@yahoo.fr

devoted to chaos by many scientist is due to the fact that this new phenomenon appears in various fields, from mathematics, physics, biology, and chemistry, to engineering, economics and medicine. Consequently, there are many opportunities for application of chaos. For example, in physics chaos has been used to refine the understanding of planetary orbits, to reconceptualize quantum level processes, and to forecast the intensity of solar activity. In engineering, chaos has been used in building of better digital filters, and to model the structural dynamics in such structures as buckling columns. In medicine, it has been used to study cardiac arrhythmias and patterns of disease communication. In psychology, it has been used to study mood fluctuations, the operation of the olfactory lobe during perception, and patterns of innovation in organizations. In economics it is being used to find patterns and develop new types of econometric model for the stock market to variations in cotton prices. There are also many opportunities for exploitation of chaos: synchronized chaos, mixing with chaos, encoding information with chaos, anti-control of chaos, tracking of chaos and targeting of chaos. An important class of systems in general and in particular oscillators who presented a complex or chaotic behavior can be determined on the basis of nonlinear damping. Such damping can, in some systems, change the sign depending on velocity or displacement values, and provide excitation energy to the examined system. These, so called, self-excited damping terms are often used to describe systems with dry friction, bearings lubricated by a thin layer of oil, shimming in vehicle wheels or chatter in a cutting process [1, 2], [5]-[8] and [16, 17]. In Ref. [27], the authors have studied with considerable detail the effects of the damping level on the resonance response of the steady-state solutions and in the basin bifurcation patterns of the escape oscillator. In particular they analyzed the effect of using different damping levels and how this contributes to the erosion of the safe areas in phase space, and they also provide a comprehensive global picture of the main bifurcation boundaries. More recently such a nonlinear damping force has also been considered [18] in modelling of a modern vehicle suspension system due to electro- or magneto-rheological fluid damping where it is causing a hysteretic effect. In this model [18] the authors used a self-excited term of the Rayleigh and the Duffing type with a double well potential. Parametric excitation occurs in a wide variety of engineering application (Refs. [9]-[13]). In this vein, we propose to study in this paper regular and chaotic behavior of the modified Rayleigh-Duffing oscillator whose equation is the form Eq. (1). This equation which having nonlinear dissipative terms and parametric excitation term can be used to model some systems such as Brusselator, Selkov, rolling response, certain *MEMS* systems... ([5]-[8], [14], and [20]- [23]).

The paper is organized as follows: In Section 2, we describe the model. Section 3 deals with the amplitude of the forced harmonic oscillatory states, using the harmonic balance method [2]. Section 4 addresses the phase portraits, largest

Lyapunov exponent and the bifurcation diagrams from which a concluding remark can be made in connection to the tendency of the system to have quasiperiodic, nonperiodic evolutions and chaotic one according to the choice of initial conditions which match with the basin of attraction found. The last section devoted to the conclusion will point out the contribution of nonlinear damping terms and parametric excitation term which modified Ordinary Rayleigh-Duffing oscillator in both regular and chaotic behaviour of oscillations of this system.

2 Model

In this paper, we consider following Modified Rayleigh-Duffing oscillator.

$$\ddot{x} + \epsilon\mu(1 - \dot{x}^2)\dot{x} + \epsilon\beta\dot{x}^2 + \epsilon k_1\dot{x}x + \epsilon k_2\dot{x}^2x + (\gamma + \alpha \cos \Omega t)x + \lambda x^3 = F \cos \Omega t, \quad (1)$$

where $\epsilon, \mu, \beta, k_1, k_2, \gamma, \lambda, F$ and Ω are parameters. Physically, μ, k_2, β and k_1 represent respectively pure, unpure cubic and pure, unpure quadratic nonlinear damping coefficient terms, α and F are the amplitudes of the parametric and external periodic forcing, and $\sqrt{\gamma}$ and Ω are respectively natural and external forcing frequency. Moreover λ characterizes the intensity of the nonlinearity and ϵ is the nonlinear damping parameter control. The nonlinear damping term corresponds to the Modified Rayleigh oscillator, while the nonlinear restoring force corresponds to the Duffing oscillator.

This oscillator is used to modelize the following phenomena: A El Niño Southern Oscillation (*ENSO*) coupled tropical ocean-atmosphere weather phenomenon in which the state variables are temperature and depth of a region of the ocean called the thermocline (where the annual seasonal cycle is the parametric excitation and the model exhibits a Hopf bifurcation in the absence of parametric excitation) ([20], [21]), a *MEMS* device consisting of a $30\mu m$ diameter silicon disk which can be made to vibrate by heating it with a laser beam resulting in a Hopf bifurcation (where the parametric excitation is provided by making the laser beam intensity vary periodically in time) ([22], [23]), the rolling response ([5]-[8]) etc. For examples, the nonlinear ship rolling response and nonlinearly damped universal uscape oscillator can be rewritten as follow:

$$\ddot{x} + \sum_{p=1}^n c_p \dot{x} |\dot{x}|^{p-1} + \sum_{j=1}^m a_j x^j = F \cos \Omega t, \quad (2)$$

where c_p is the nonlinear damping and a_p restoring coefficients. In the ship rolling case, A. Francescutto and G. Contento [5] are used experimental results and parameter identification technique to study bifurcations in ship

rolling, application of the extended Melnikov's method are used by W. Wu and L . McCue [7] de for single-degree-of-freedom vessel roll motion. In the other hand MIGUEL A. F. SANJUÀN (in Ref.[28]) analyzed the effect of nonlinear damping on the universal escape oscillator. Another examples, consider the modified Rayleigh-Duffing oscillator equation which describes the glycolytic reaction catalized by phosphofructokinase, namely the Selkov equations and abstract trimolecular chemical reaction namely Brusselator oscillator [14]:

One of these processes is simple classical two-variable model which describes glycolytic reaction catalized by phosphofructokinase, namely the Selkov equations

$$\begin{aligned}\frac{dx}{dt} &= v - xy^2, \\ \frac{dy}{dt} &= xy^2 - wy,\end{aligned}\tag{3}$$

and another is the Brusselator which describes an abstract trimolecular chemical reaction

$$\begin{aligned}\frac{dx}{dt} &= A + xy^2 - (B + 1)x, \\ \frac{dy}{dt} &= Bx - xy^2,\end{aligned}\tag{4}$$

For the Selkov model $\lambda = v^2w^{-2} - w$, $\lambda' = (z_0w - 3v)/w^2$, $\lambda'' = w^{-2}$, $k = v^{-1}\Omega = v/\sqrt{w}$, where $z_0 = w^2/v + v/w$. For the Brusselator $\lambda = 1 + A^2 - B$, $\lambda' = (B - 2A^2)/A$, $\lambda'' = 1$, $k = A^{-1}$, $\Omega = A$ and $z_0 = (B + A^2)/A$. In both cases $\xi = x + y - z_0$ is a deviation from the equilibrium concentration. With these conditions, the two last systems can be rewritten

$$\frac{d^2\xi}{dt^2} + \tilde{\lambda}\frac{d\xi}{dt} + \tilde{\lambda}''\left(\frac{d\xi}{dt}\right)^2 + \tilde{\lambda}'\left(\frac{d\xi}{dt}\right)^3 + \Omega^2\left(1 - k\frac{d\xi}{dt}\right)^2\xi = 0.\tag{5}$$

Perturbing this system by Duffing force, parametric excitation force and external sinusoidal forced, we obtained the parametric dissipative modified Rayleigh-Duffing oscillator which is expressed by Eq. (1). We will study the harmonic vibration, the bifurcation and transition to chaos of the system. The effects of the nonlinear damping, the parametric excitation amplitude and the external forcing amplitude will be seeked. Through this work, we will find our modified Rayleigh-Duffing oscillator regular and chaotic behaviors.e

3 Harmonic oscillatory states

Assuming that the fundamental component of the solution and the external excitation have the same period, the amplitude of harmonic oscillations can be tackled using the harmonic balance method [2]. For this purpose, we express its solutions as

$$x = A \cos(\Omega - \psi) t + \xi\tag{6}$$

where A represents the amplitude of the oscillations and ξ a constant.

Inserting this solution Eq.(6) in Eq.(1) and equating the constants and the coefficients of $\sin \Omega t$ and $\cos \Omega t$, we have

$$\begin{aligned} & [-A\Omega^2 - \frac{1}{2}\epsilon\beta\Omega^2 A^2 + \alpha\xi + \gamma A + 3\lambda\xi^2 A + \frac{3}{4}\lambda A^3 + \frac{1}{4}\epsilon k_2\Omega^2 A^3]^2 + \\ & [-\epsilon\mu\Omega A + \frac{3}{4}\mu\epsilon\Omega^3 A^3 - \epsilon k_1\Omega\xi A]^2 = F_0^2, \end{aligned} \quad (7)$$

$$\frac{1}{2}\epsilon\beta\Omega^2 A^2 + \frac{1}{2}\epsilon k_2\xi\Omega^2 A^2 + \frac{1}{2}\alpha A + \gamma\xi + \lambda\xi^3 + \frac{3}{2}\lambda\xi A^2 = 0. \quad (8)$$

If it is assumed that $|\xi| \ll |A|$, i.e that shift in $x = 0$ is small compared to the amplitude [8], then ξ^2 and ξ^3 terms can be neglected, Eq.(8) become

$$\frac{1}{2}\epsilon\beta\Omega^2 A^2 + \frac{1}{2}\epsilon k_2\xi\Omega^2 A^2 + \frac{1}{2}\alpha A + \gamma\xi + \frac{3}{2}\lambda\xi A^2 = 0. \quad (9)$$

We obtained

$$\xi = \frac{\frac{1}{2}\epsilon\beta\Omega^2 A^2 + \frac{1}{2}\alpha A}{-\gamma - \frac{1}{2}(\epsilon k_2\Omega^2 + 3\lambda)A^2}. \quad (10)$$

Substituting Eq.(10) into Eq. (7) leads us to the following nonlinear algebraic equation

$$\begin{aligned} & [-A\Omega^2 - \frac{1}{2}\epsilon\beta\Omega^2 A^2 + \gamma A + A + \frac{1}{4}(\epsilon k_2\Omega^2 + 3\lambda)A^3 + \\ & \frac{\frac{1}{2}\epsilon\alpha\beta\Omega^2 A^2 + \frac{1}{2}\alpha^2 A}{-\gamma - \frac{1}{2}(\epsilon k_2\Omega^2 + 3\lambda)A^2}]^2 + \\ & [-\epsilon\mu\Omega A + \frac{3}{4}\epsilon\mu\Omega^3 A^3 - \epsilon k_1\Omega \frac{\frac{1}{2}\epsilon\beta\Omega^2 A^2 + \frac{1}{2}\alpha A}{-\gamma - \frac{1}{2}(\epsilon k_2\Omega^2 + 3\lambda)A^2} A]^2 = F_0^2, \end{aligned} \quad (11)$$

After some algebraics manipulations, Eq. (11) can be rewritten as follow:

$$\begin{aligned} & (a^2 + f^2)A^{10} + 2abA^9 + (b^2 + 2ac + 2fg)A^8 + (2bc + 2ad + 2fh)A^7 + \\ & (c^2 + 2bd + 2ae + 2fi + g^2)A^6 + (2ed + 2be + 2gh)A^5 + \\ & (d^2 + j + h^2 + 2ce + 2gi)A^4 + (2de + 2hi)A^3 + \\ & (e^2 + i^2 + k)A^2 + l = 0, \end{aligned} \quad (12)$$

with

$$\begin{aligned} a &= -\frac{1}{8}(\epsilon k_2\Omega^2 + 3\lambda)^2, & b &= \frac{1}{4}\epsilon\beta\Omega^2(\epsilon k_2\Omega^2 + 3\lambda), \\ c &= -\frac{1}{4}(3\gamma - 2\Omega^2)(\epsilon k_2\Omega^2 + 3\lambda), & d &= \frac{1}{2}\epsilon\beta\Omega^2(\gamma + \alpha), \end{aligned}$$

$$\begin{aligned}
e &= \frac{1}{2}\alpha^2 - \gamma(\gamma - \Omega^2), & f &= -\frac{3}{8}\epsilon\mu\Omega^2(\epsilon k_2\Omega^2 + 3\lambda), \\
g &= \frac{1}{2}[\epsilon\mu\Omega(\epsilon k_2\Omega^2 + 3\lambda) - \frac{3}{2}\epsilon\mu\gamma\Omega^2 - \epsilon^2\beta k_1\Omega^3], \\
h &= -\frac{1}{2}\epsilon^2\alpha k_1\Omega, & i &= \epsilon\mu\gamma\Omega, & j &= -\frac{1}{4}F_0^2(\epsilon k_2\Omega^2 + 3\lambda)^2, \\
k &= \gamma F_0^2(\epsilon k_2\Omega^2 + 3\lambda), & l &= -F_0^2\gamma^2.
\end{aligned} \tag{13}$$

We investigate the effects of system parameters on the amplitude of oscillations A by solving Eq. (12) using the Newton-Raphson algorithm. The five first figures are the amplitude-response curves and its showing the hysteresis and jump phenomena. Fig.1 show the effect of γ on amplitude-response curve where hysteresis and jump phenomena appeared when $\gamma = -1$ and disappeared when $\gamma = 1$. Fig.2 illustrate the effect of external frequency on amplitude-response curve. Through this figure we notice that the hysteresis phenomenon disappeared when the external frequency increasing. Figs.3 (a), (b), (c) and (d) illustrate the effects of damping coefficients μ, k_2, k_1 and β respectively while the effects of the cubic nonlinear Duffing coefficient and amplitude of parametric excitation are shown in Figs.3 (e) and (f) respectively. Through these figures we noticed that when the cubic nonlinear damping coefficients μ and k_2 increasing, the hysteresis and jump phenomena disappear (see Figs. 3 (a), (b)) while these two phenomena became more several but amplitude of harmonic oscillations decreases when the pure quadratic nonlinear damping coefficient is increased (see. We notice that 3 (c)). The effect of unpure nonlinear quadratic damping parameter k_1 is not significated (see 3 (d)). One can notice that as λ decreases, the jump and hysteresis phenomenon disappear (see 3 (f)). The topology of jump and hysteresis phenomenon curves is well influenced by the parametric excitation amplitude as shown in Fig. 3 (a). In that figure, the amplitude-response curves are plotted for different value of α . One notices that as increases, the topology of these two phenomenon are very modified. The behavior of the amplitude of this system oscillations is investigated when the external frequency Ω varies and the results are plotted in Fig. 4 where analytical resonance curves $A(\Omega)$ of the model is shown. The resonance obtained from Fig.4 is also affected by the nonlinear damping parameters, parametric excitation amplitude and external forced amplitude (see Figs. 5, 6). Thereby, the observed resonant state obtained for a set of parameters can be destroyed according to the value taken by these parameters. For instance, when the damping coefficients μ, k_1, β increasing the frequency-response curve is destroyed, the peak value of resonance amplitude is decreased and we noticed that the resonance disappear (see Figs 5 (a), (c), (d)). Fig.4 (b) show that when k_2 is increased the peak value of resonance amplitude increased while the resonance frequency decreased. Through Figs. 6 (a), (b), (c) we noticed also that the parameter λ have the same effect that μ and k_1 on the frequency-response curve (see

Fig.6 (a)) while when α increasing the resonance frequency is decreased (see 6 (b)) and the frequency-response curve become largest when the external forced amplitude is increased but the resonance frequency is not affected (see 6 (c)).

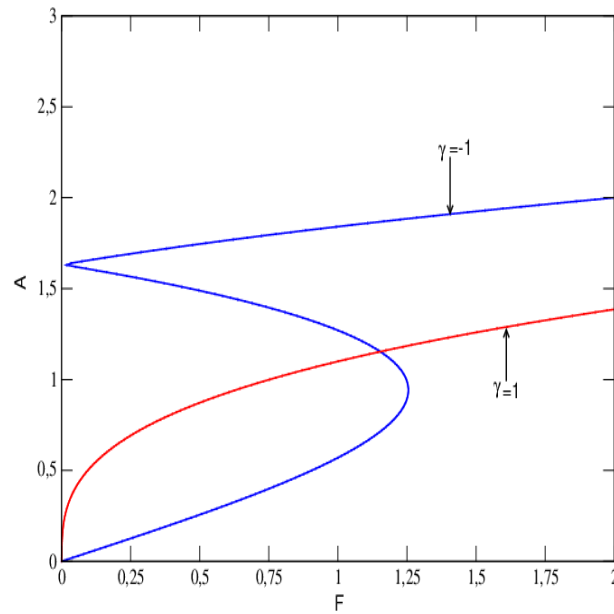


Figure 1: Effects of γ on the amplitude-response curves with the parameters $\alpha = 0$, $\beta = 0.5$, $k_1 = 0.5$, $k_2 = 0.5$, $\mu = 0.5$, $\lambda = 1$ and $\Omega = 1$.

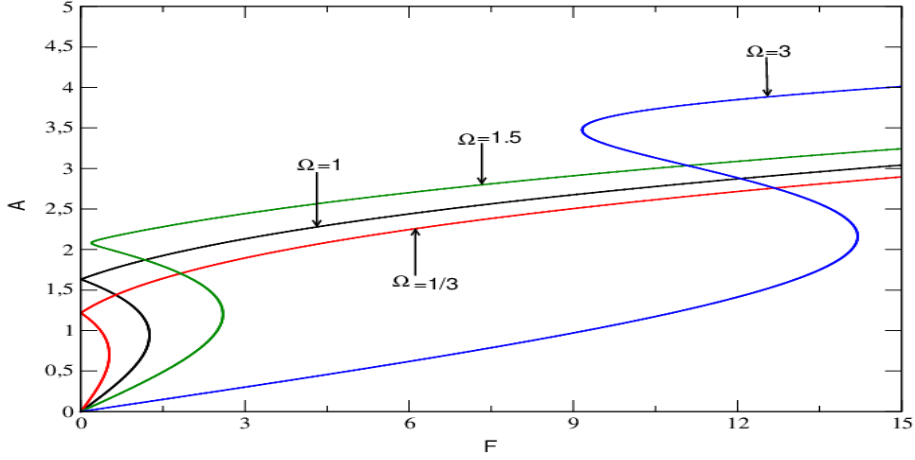


Figure 2: Effects of Ω on the amplitude-response curves with $\gamma = -1$, and the parameters of Fig.1.

4 Bifurcation and transition to chaos

Our aim in this section is to investigate the way under which chaotic motions arise in the model described by Eq. (1) for resonant states since they are of interest in (*ENSO*), *MEMS* device consisting of a $30\mu m$ diameter silicon disk which can be made to vibrate by heating, Brusselator and Selkov oscillators etc. For this purpose, we numerically solve this equation using the fourth-order Runge Kutta algorithm [26] and plot the resulting bifurcation diagrams and the variation of the corresponding largest Lyapunov exponent as the amplitude F , the parameters of nonlinearity $\mu, \beta, k_1, k_2, \lambda$ and γ are varied. The stroboscopic time period used to map various transitions which appear in the model is $T = \frac{2\pi}{\Omega}$. The largest Lyapunov exponent which is used here as the instrument to measure the rate of chaos in the system is defined as

$$Lya = \lim_{t \rightarrow \infty} \frac{\ln \sqrt{dx^2 + d\dot{x}^2}}{t} \quad (14)$$

where dx and $d\dot{x}$ are respectively the variations of x and \dot{x} . Initial condition that we are used in the simulations of this section is $(x_0, \dot{x}_0) = (1, 1)$. In order to have an idea about the system behavior as predicted by the bifurcation diagram, various phase portraits for several different values of F chosen in the above mentioned regions are plotted in Figs. 10, 11 and 12 using respectively the parameters of Figs. 7, 8 and 9. It should be emphasized from Figures 7, 8 and 9 that there are some domains where the Lyapunov exponent does not match very well the regime of oscillations expected from the bifurcation diagram. Far from being an error which

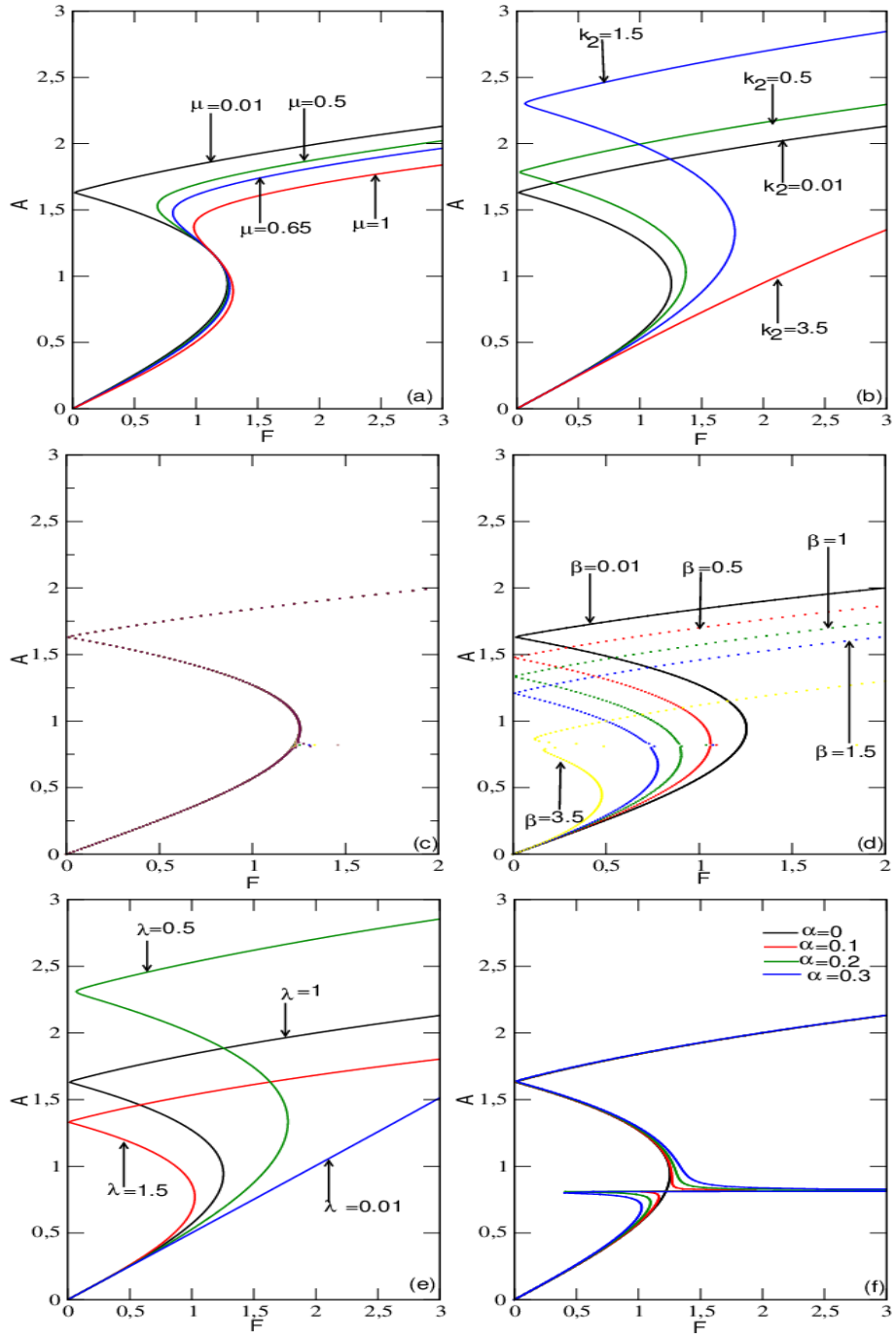


Figure 3: (a) : Effect of μ , (b) : effect of k_2 , (c) : effect of k_1 , (d) : effect of β , (d) : effect of λ and (e) : effect of α on the amplitude-response curves with $\Omega = 1$, and the parameters of Fig. 1.

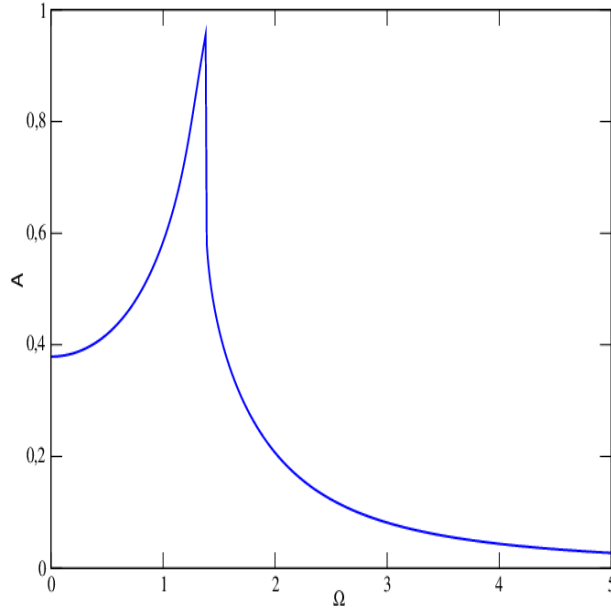


Figure 4: Frequency-response curves with the parameters $\alpha = 0, \beta = 0.5, k_1 = 0.5, k_2 = 0.5, \mu = 0.25, \lambda = 1, \gamma = 1$ and $F = 0.65$.

has occurred from the numerical simulation process, such a behavior corresponds to what is called the intermittency phenomenon. Therefore, within these intermittent domains, the dynamics of the model can not be predicted. For instance, some forecasted period-1 and quasiperiodic motions from the bifurcation diagram are not confirmed by the Lyapunov exponent. Indeed, phase portraits display rather quasiperiodic, nonperiodic or chaotic motions. Due to the high sensitivity of the model to initial conditions, basins of chaoticity (where for any choice of initial conditions that belongs to the shaded area will lead the system to chaotic states while if the initial conditions are chosen in the non-shaded area, the system will display periodic or quasi-periodic states) are also checked in primary, superharmonic and subharmonic resonant states (see Figs. 13, 14 and 15. respectively). From these figures, we conclude that chaos is more abundant in the superharmonic resonant states than in the primary and subharmonic resonances. This confirms what has been obtained through their bifurcation diagrams and Lyapunov exponent. To show how the parameters of modified nonlinearity can influence the chaotic motion in the model, the Lyapunov exponent has also been plotted versus μ, k_1, k_2, β and parametric excitation amplitude with the parameters of Fig. 7 and the following results are observed: As

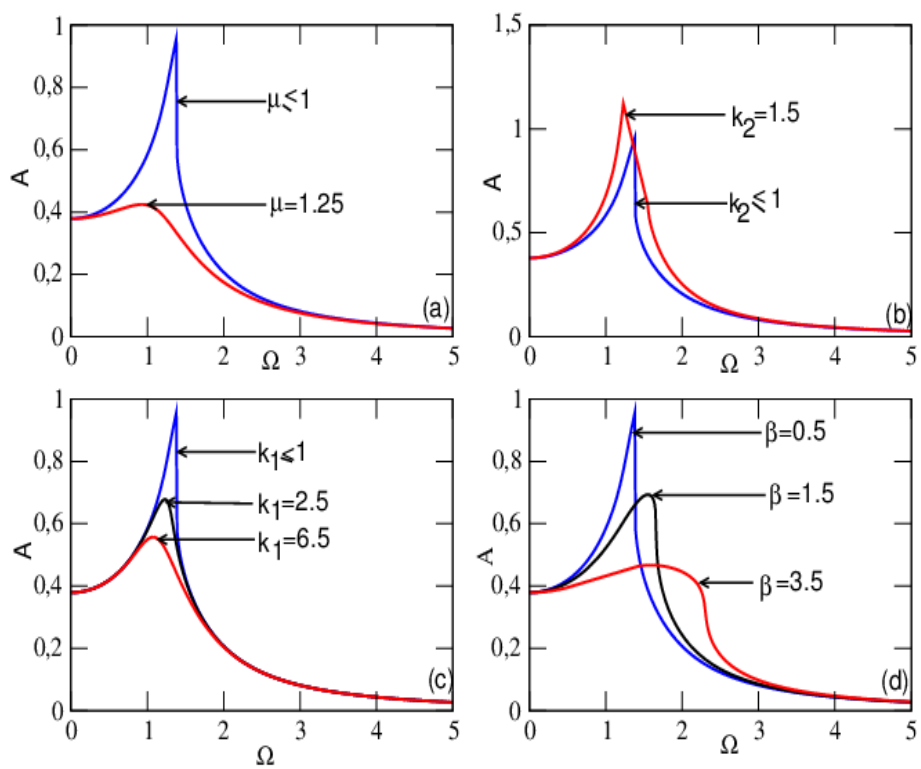


Figure 5: Effects of damping on frequency-response curves with the parameters of Fig.6 (a) effect of μ , (b) effect of k_2 , (c): effect of k_1 and (d) effect of β .

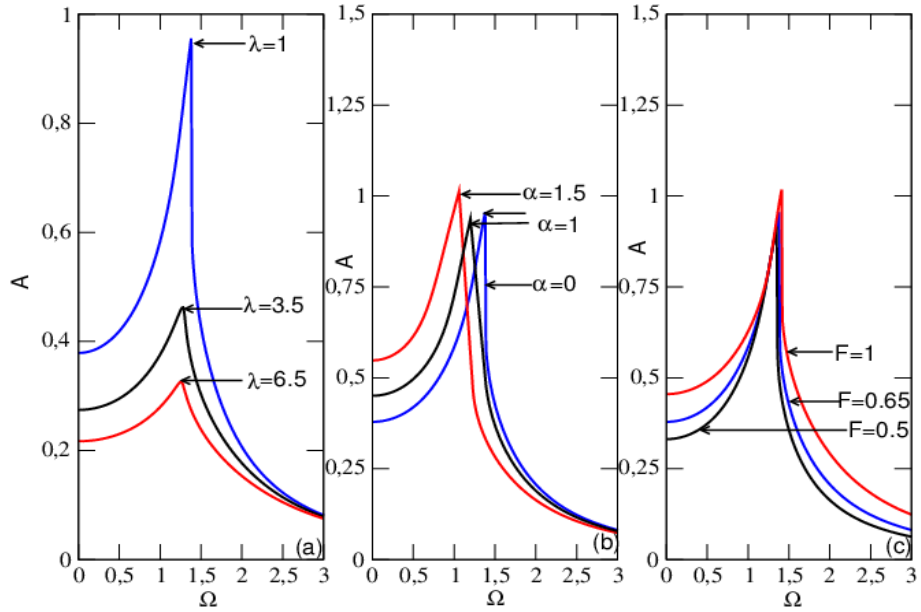


Figure 6: Effects of other on parameters frequency-response curves with the parameters of Fig.6 (a) effect of λ , (b) effect of α , (c): effect of amplitude of external forced F .

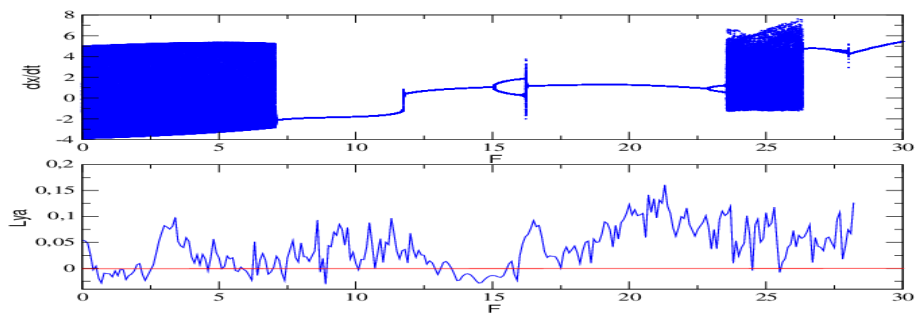


Figure 7: Bifurcation diagram (upper frame) and Lyapunov exponent (lower frame) versus the amplitude F with parameters for $\alpha = 0.3, \beta = 0.05, k_1 = 0.05, k_2 = 0.05, \mu = 0.0001, \lambda = 1, \gamma = 1$ and $\Omega = 1$

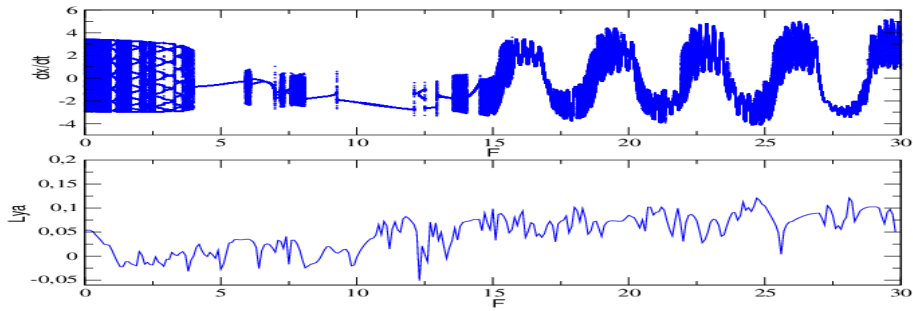


Figure 8: Bifurcation diagram (upper frame) and Lyapunov exponent (lower frame) versus the amplitude F with parameters $\alpha = 0.3, \beta = 0.05, k_1 = 0.05, k_2 = 0.05, \mu = 0.0001, \lambda = 1, \gamma = 1$ and $\Omega = 1/3$

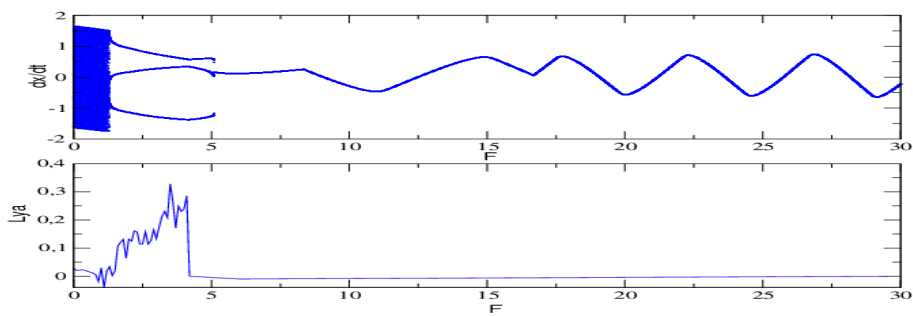


Figure 9: Bifurcation diagram (upper frame) and Lyapunov exponent (lower frame) versus the amplitude F with parameters $\alpha = 0.3, \beta = 0.5, k_1 = 0.5, k_2 = 0.5, \mu = 0.0001, \lambda = 1, \gamma = 1$ and $\Omega = 3$

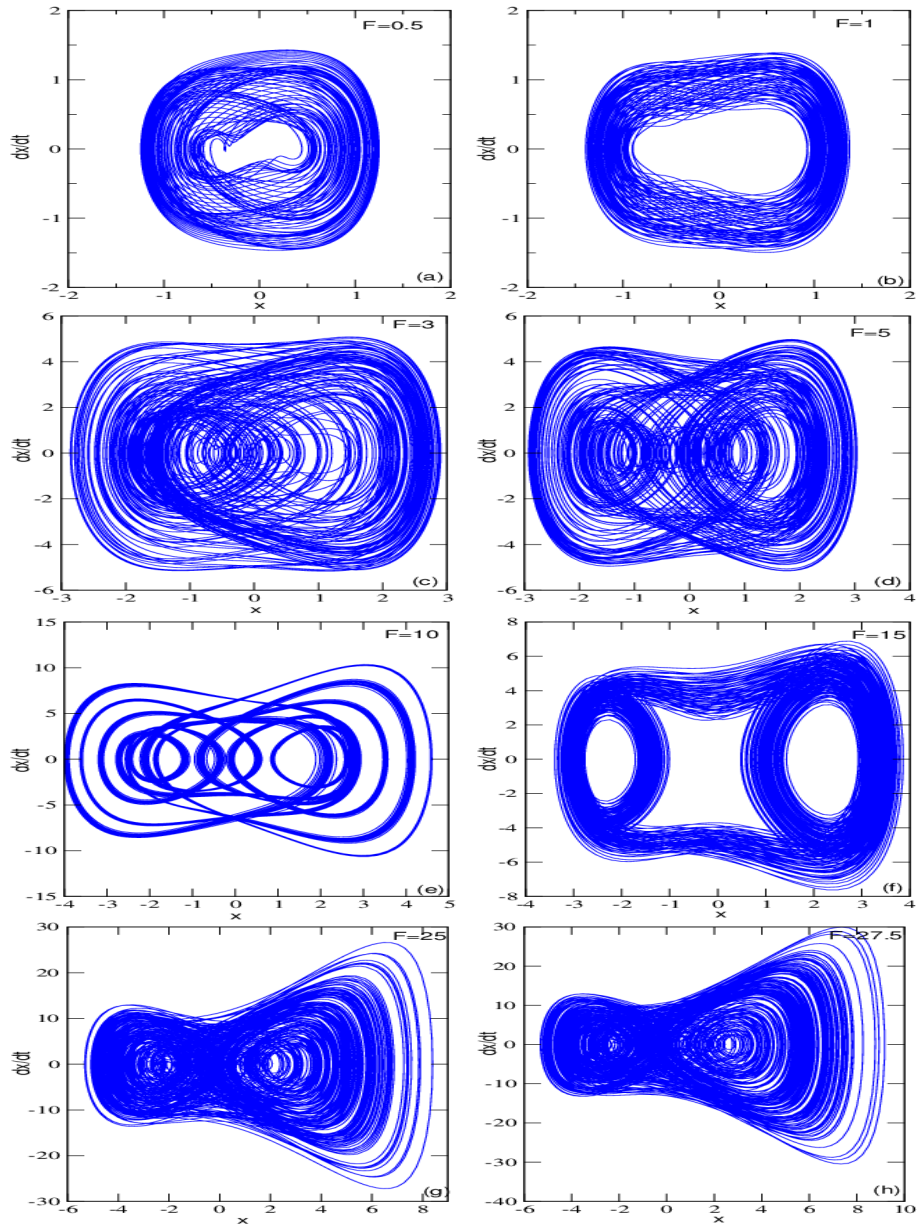


Figure 10: Various phase portraits for several different values of F with the parameters of Fig. 7.

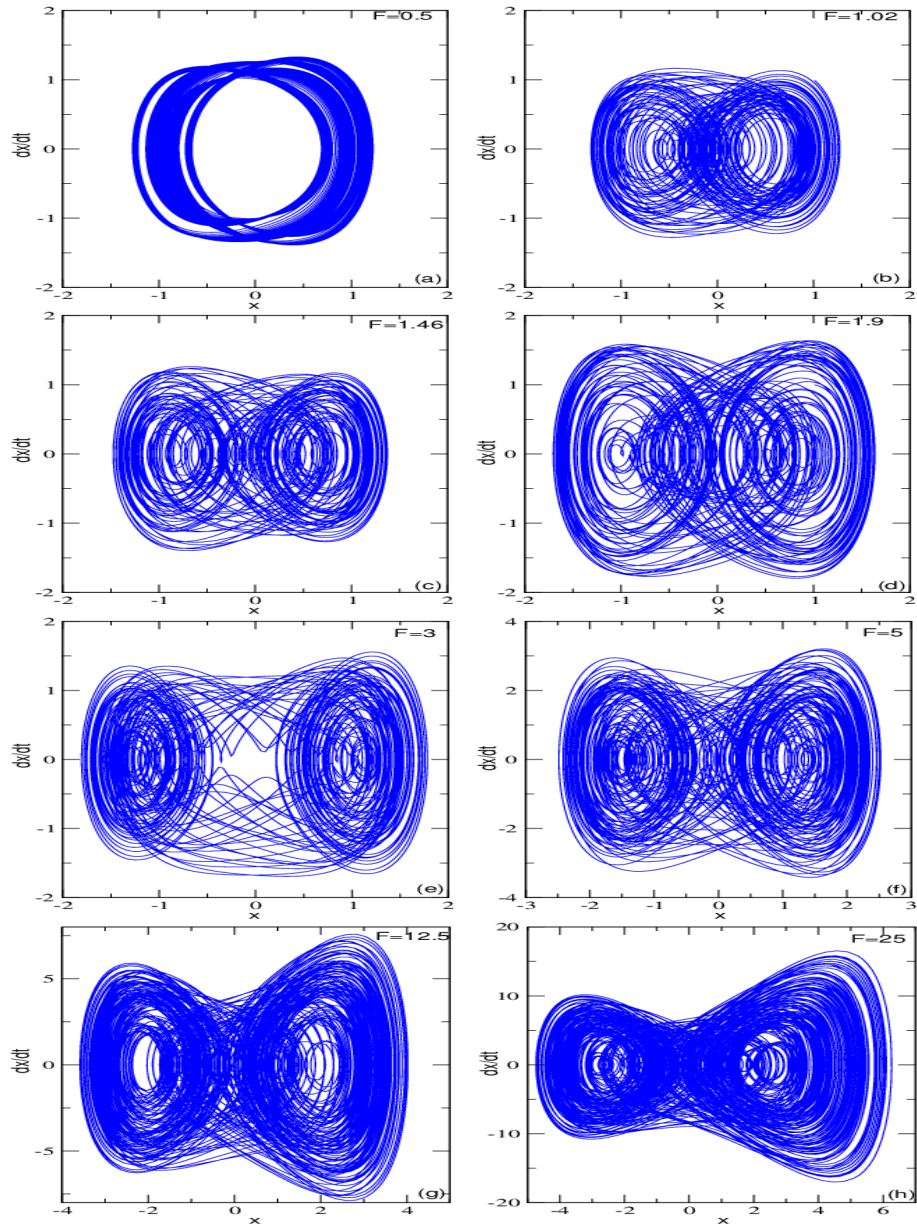


Figure 11: Various phase portraits for several different values of F with the parameters of Fig.8.

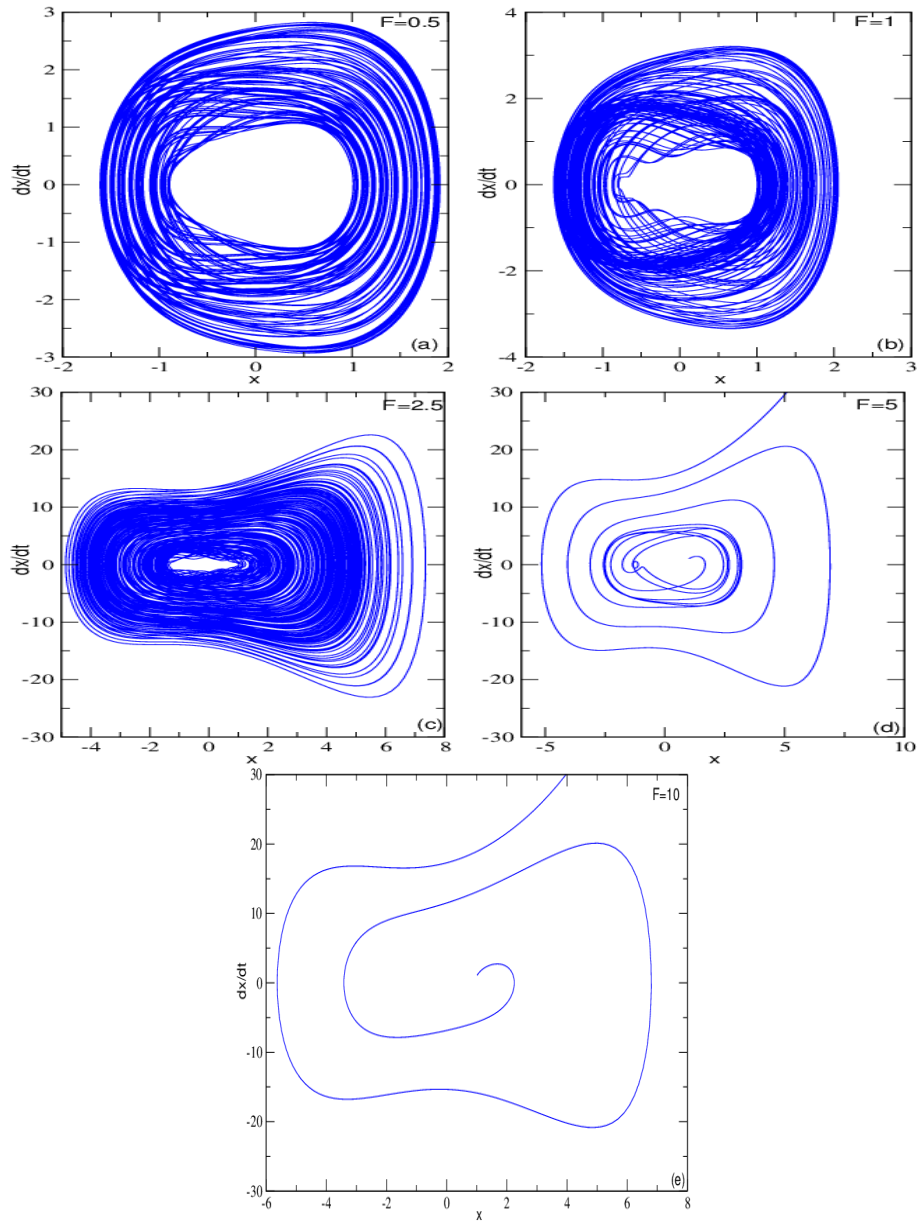


Figure 12: Various phase portraits for several different values of F with the parameters of Fig.9.

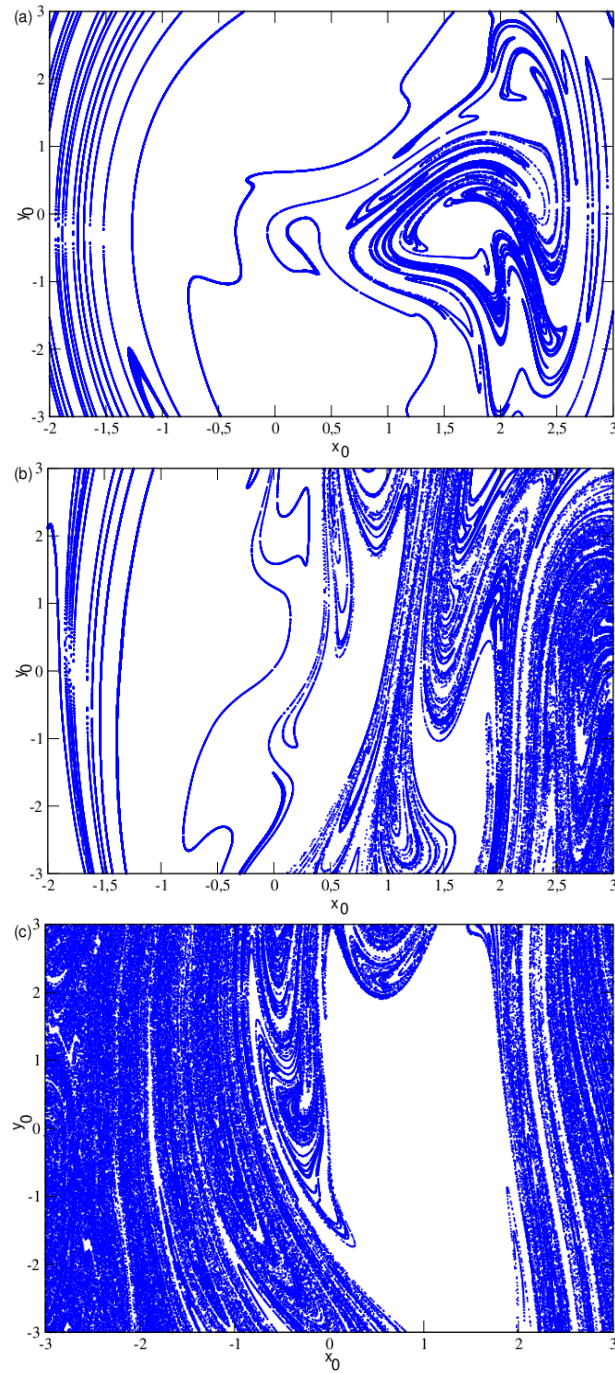


Figure 13: Various basin of chaoticity in the primary resonant state with parameter of and (a) $F = 5$, (b) $F = 10$ and (c) $F = 15$.

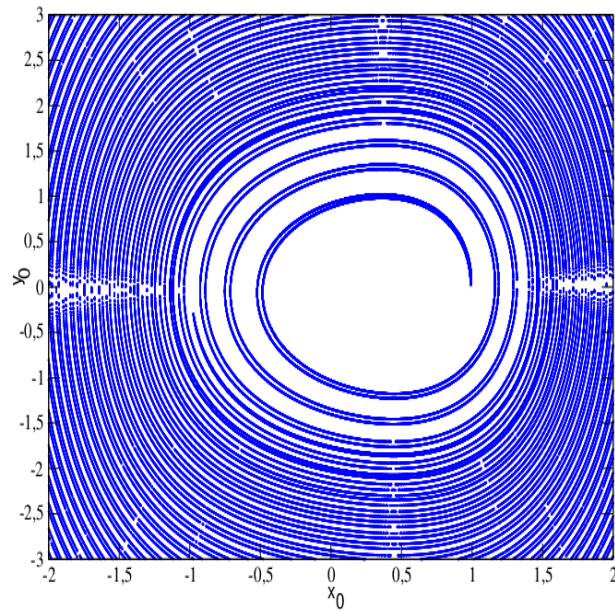


Figure 14: Basin of chaoticity in the superharmonic resonant state.

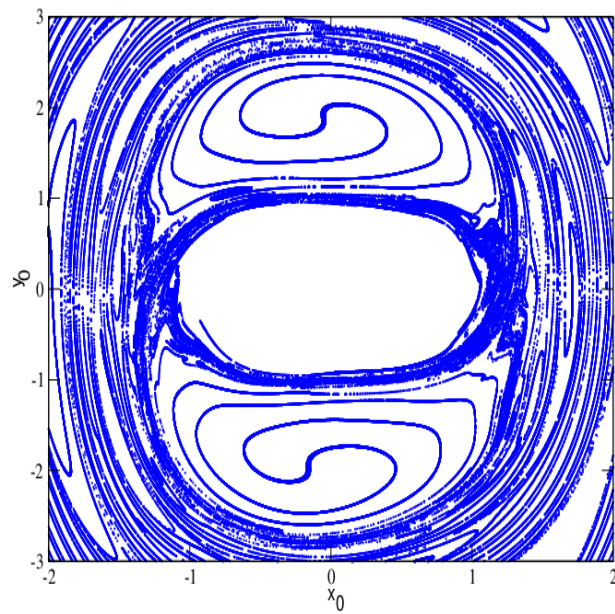


Figure 15: Basin of chaoticity in the subharmonic resonant state.

5 Conclusion

We have investigated regular and chaotic behaviors of modified Rayleigh-Duffing oscillator. The amplitude of harmonic amplitude is found by using the balance harmonic method. It is obtained the hysteresis and jump phenomena and resonance phenomenon have appeared in (Ω, A) space. It is found that the nonlinear damping and parametric excitation amplitude affected severaly the amplitude and frequency of resonance curve. Various bifurcation structures showing different types of transitions from quasi-periodic motions to periodic, unperiodic and chaotic motions have been drawn and the influences of different parameters on these motions have been study. It is noticed that chaotic motions have been controlled by the parameters $\mu, \beta, k_1, k_2, \alpha$, and external frequency. The results of basin attraction show a way to predict initial conditions which regular and chaotic behaviors are obtained. This could be helpful for experimentalists who are interested in trying to stabilize such a system with differents parameters or initial conditions . For practical interests, it is useful to develop tools and to find ways to control or suppress such undesirable regions. This will be also useful to control high amplitude of oscillations obtained and which are generally source of instability in systems which modeled by this modified Rayleigh-Duffing oscillator equation.

Acknowlegments

The authors thank IMSP-UAC and Benin gorvernment for financial support. We also thank Laurent Hinvi for his fruitfull suggestions and Professor Paul Wofo for his suggestions and collaboration.

References

- [1] Nayfeh, A. H., and Mook, D. T., 1979, *Nonlinear Oscillations*, Wiley, New York.
- [2] Hayashi. C., 1964, *Nonlinear Oscillations in Physical Systems*, McGraw-Hill, New York.
- [3] Chedjou,J. C., Fostin, H. B., and Wofo, P., 1997, "Behavior of the van der Pol Oscillator with Two External Periodic forces",Phys. Scr., 55,pp,390-393. DEA de Physique des liquides. Paris VI- Ecole Polytechnique.
- [4] Carrol, T. L., 1995, "Communicating With Use of filtered, Synchronized, Chaotic Signals." IEEE Trans, Circuits syst.,I: Fundam. Theory Appl.,42,pp. 105-110.

- [5] Alberto Francescutto, Giorgio Contento, *Bifurcations in ship rolling: experimental results and parameter identification technique*, Ocean Engineering 26 (1999) 1095–1123.
- [6] K.W. Holappa, J.M. Falzarano *Application of extended state space to nonlinear ship rolling*, Ocean Engineering 26 (1999) 227–240.
- [7] Wan Wu, Leigh McCue, *Application of the extended Melnikov's method for single-degree-of-freedom vessel roll motion*, Ocean Engineering 35 (2008) 1739–1746.
- [8] R. A. Mahaffey, *Physics of Fluids* 19, 1837 (1976).
- [9] K. Ostrikov and S. Xu, *Plasma-aided Nanofabrication: from Plasma Sources to Nanoassembly* (John Wiley Sons, Weinheim, 2007), pp. 149 – 280.
- [10] H. G. Enjieu Kadji, J. B. Chabi Orou and P. Wofo, *Physica Scripta* (In Press) (2007).
- [11] H. G. Enjieu Kadji, B. R. Nana Nbandjo, J. B. Chabi Orou, and P. K. Talla, *Nonlinear dynamics of plasma oscillations modeled by an anharmonic oscillator* (2007).
- [12] S.H. Strogatz, *Nonlinear dynamics and chaos with applications to physics, chemistry and engineering*, (Westview Press, Cambridge, 1994), Sec. 1.2.
- [13] R. Yamapi, M.A. Aziz-Alaoui, *Vibration analysis and bifurcations in the self-sustained electromechanical system with multiple functions*, Communications in Nonlinear Science and Numerical Simulation 12(2007)1534 – 1549.
- [14] Darya V. Vervevko and Andrey Yu. Verisokin, *Application of He's method to the modified Rayleigh equation*, Discrete and Continuous Dynamical Systems, Supplement 2011, pp. 1423–1431.
- [15] Aubin, K., Zalalutdinov, M., Alan, T., Reichenbach, R. B., Rand, R. H., Zehnder, A., Parpia, J. and Craighead, H. G., *Limit Cycle Oscillations in CW Laser-Driven NEMS*, Journal of Micro-electrical mechanical System 13:1018-1026, 2004.
- [16] Zalalutdinov, M., Olkhovets, A., Zehnder, A., Ilic, B., Czaplewski, D. and Craighead, H. G., *Optically pumped parametric amplification for micro-mechanical systems*, Applied Physics Letters 78:3142-3144, 2001.

- [17] Rand, R. H., Ramani, D. V, Keith, W. L. and Cipolla, K. M., *The quadratically damped Mathieu equation and its application to submarine dynamics*, Control of Vibration and Noise: New Millennium 61:39-50, 2000.
- [18] Wirkus, S., Rand, R. H. and Ruina, A., *How to pump a swing*, The College Mathematics Journal 29:266-275, 1998.
- [19] Zhehe Y., Deqing M., Zichen C., *Chatter suppression by parametric excitation: Model and experiments*, Communications in Nonlinear Science and Numerical Simulation 330:2995-3005, 2011.
- [20] Wang, B. and Fang, Z.,
'Chaotic Oscillations of Tropical Climate: A Dynamic System Theory for ENSO', Journal of Atmospheric Sciences 53:2786-2802, 1996.
- [21] Wang, B., Barcilon, A. and Fang, Z.,
'Stochastic Dynamics of El Nino- Southern Oscillation', Journal of Atmospheric Sciences 56:5-23, 1999.
- [22] Zalalutdinov, M., Parpia, J.M., Aubin, K.L., Craighead, H.G., T.Alan, Zehnder, A.T. and Rand, R.H., *Hopf Bifurcation in a Disk-Shaped NEMS*, Proceedings of the 2003 ASME Design Engineering Technical Conferences, 19th Biennial Conference on Mechanical Vibrations and Noise, Chicago, IL, Sept. 2-6, paper no.DETC2003-48516, 2003 (CD-ROM).
- [23] Pandey, M., Rand, R. and Zehnder, A., *'Perturbation Analysis of Entrainment in a Micromechanical Limit Cycle Oscillator'*, Communications in Nonlinear Science and Numerical Simulation, available online, 2006.
- [24] Tina Marie Morrison, *Three problems in nonlinear dynamics with 2:1 parametric excitation*, Ph.D. Cornell University 2006.
- [25] A. H. Nayfeh, *Introduction to perturbation techniques*, (John Wiley and Sons, New York, 1981), Sec.4.5.
- [26] N. Piskunov, *Calcul Différentiel et intégral*, Tome II, 9^e edition, MIR, Moscou (1980).
- [27] Soliman, M. S. and Thompson, J. M. T. *The effect of damping on the steady state and basin bifurcation patterns of a nonlinear mechanical oscillator*, Int. J. Bifurcation and Chaos 2, 81–91 (1992).
- [28] Sanjuan MAF. *The effect of nonlinear damping on the universal escape oscillator*. Int J Bifurcat Chaos 1999;9:735.